J. Org. Chem. **1994,** *59,* 2537–2545

The Influence of Inter- and Intramolecular Hydrogen Bonding upon the Structure and Photochemistry of 3-(2-Pyridyl)propenamides

Frederick D. Lewis* and Beth A. Yoon

Department of Chemistry, Northwestern University, Evanston, Illinois 60208-3113

Received November 29, 1993•

The molecular structures and photochemical behavior of (*E*)- and (*Z*)-*N*-methyl-3-(2-pyridyl)-propenamide have been investigated in the solid state and in solution. While the molecular conformation of the thermodynamically more stable *E* isomer is independent of phase or solvent, the conformation of the *Z* isomer is dependent upon its environment, adopting an s-trans intramolecular hydrogen-bonded conformation in chlorocarbon solvents, an s-cis conformation in methyl sulfoxide solution, and an orthogonal intermolecular hydrogen-bonded conformation in the solid state. The electronic structure of these molecules has been investigated using the semiemperical INDO/S-SCF-CI (ZINDO) algorithm. The two lowest energy absorption bands are attributed to allowed $\pi \rightarrow \pi^*$ transitions; however, the existence of lower energy singlet n,π^* states is predicted. Neither isomer undergoes photoisomerization in the solid state. Photoisomerization of the *E* isomer is efficient in nonpolar solvents but occurs with decreased efficiency in solvents which are good hydrogen bond acceptors. The *Z* isomer undergoes photoisomerization only in strong hydrogen bond acceptor solvents which disrupt the intramolecular hydrogen bond. Thus, either inter- or intramolecular hydrogen bonding can influence the efficiency of photoisomerization. Similar results are obtained with several related N-substituted 3-(2-pyridyl)propenamides. These results provide the first example of counterthermodynamic one-way $E \rightarrow Z$ photoisomerization based upon intramolecular hydrogen bonding.

Introduction

The effect of intramolecular hydrogen bonds on molecular conformation is a topic of continuing interest in organic chemistry.[1] Intramolecular hydrogen bonds can influence the thermal equilibrium between configurational isomers. The *Z* isomers of enols, enamines, and enamides capable of forming 6-membered intramolecular hydrogen bonds can be more stable than their *E* isomers in solvents which do not disrupt the hydrogen bond.[2] Intramolecular hydrogen bonds can also influence the photochemical behavior of organic molecules.[3-7] The vinylpyridine derivatives **1–3** have been reported to undergo one-way $E \rightarrow Z$ photoisomerization,[4a,5,7] although later it was reported that (*Z*)-**1** does undergo photoisomerization albeit less efficiently than (*E*)-**1**.[4b] In the case of **1** and **2**, the *Z* isomer is thermodynamically more stable than the *E* isomer and absorbs at longer wavelength. Thus, photoisomerization converts the thermodynamically less stable isomer to the more stable one (eqs 1 and 2), as is the case in most other one-way photoisomerization reactions. However, the one-way $E \rightarrow Z$ photoisomerization of 3-(2-pyridyl)propenamide (**3**) is unusual in that the thermodynamically more stable *E* isomer is quantitatively converted to the less stable *Z* isomer (eq 3).[7] We report here the results of our detailed investigation of the molecular and electronic structure of (*E*)- and (*Z*)-**3** and the effects of structure and solvent upon the photoisomerization of 3-(2-pyridyl)propenamides **3–6**. Comparison of these with results with those for *N*-methyl-3-(3-pyridyl)propenamide (**7**) and *N*-methylcinnamamide (**8**), neither of which can form intramolecular

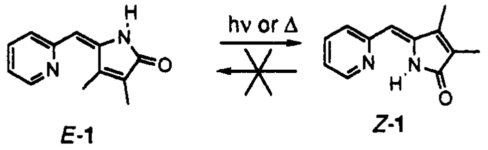

(1)

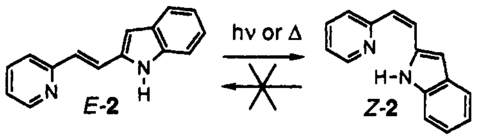

(2)

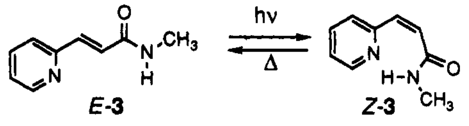

(3)

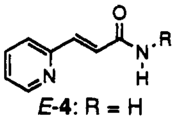

E-4: R = H
E-5: R = COCH$_3$
E-6: R = Ph

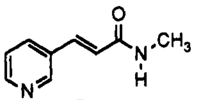

E-7

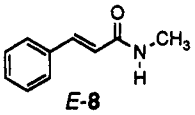

E-8

• Abstract published in *Advance ACS Abstracts*, April 1, 1994.

[1] (a) Etter, M. C. *Acc. Chem. Res.* **1990,** *23,* 120. (b) Rebek, J., Jr. *Angew. Chem., Int. Ed. Engl.* **1990,** *29,* 245. (c) Williams, D. H. *Aldrichchim. Acta* **1991,** *24,* 71. (d) Jorgensen, W. L. *Chemtracts Org. Chem.* **1991,** 91.

[2] (a) Sandström, J. *Topics Stereochem.* **1983,** *14,* 83. (b) Grande, K. D.; Rosenfeld, S. M. *J. Org. Chem.* **1980,** *45,* 1626. (c) McMullen, C. H.; Stirling, C. J. M. *J. Chem. Soc. B* **1966,** 1217. (d) Herbig, K.; Huisgen, R.; Huber, H. *Chem. Ber.* **1966,** *99,* 2546.

[3] (a) McMullen, C. H.; Stirling, C. J. M. *J. Chem. Soc. B* **1966,** 1217. (b) Herbig, K.; Huisgen, R.; Huber, H. *Chem. Ber.* **1966,** *99,* 2546. (c) Henning, H.-G.; Bandlow, M.; Jedrych, Y.; Berlinghoff, R. *J. Prakt. Chem.* **1978,** *320,* 945.

[4] (a) Lightner, D. A.; Park, Y.-T. *J. Heterocycl. Chem.* **1977,** *14,* 415. (b) Falk, H.; Neufingerl, F. *Monatsh. Chem.* **1979,** *110,* 1243–55. (c) Falk, H.; Grubmayr, K. *Monatsh. Chem.* **1977,** *108,* 625. (d) de Groot, J. A.; Jansen, H.; Fokkens, J. R.; Lugtenburg, J. *Recl. Trav. Chem. Pays-Bas.* **1983,** *102,* 114.

[5] (a) Eenkhoorn, J. A.; de Silva, S. O.; Snieckus, V. *Can. J. Chem.* **1972,** *51,* 792. (b) Arai, T.; Iwasaki, T.; Tokumaru, K. *Chem. Lett.* **1993,** 691.

[6] Lewis, F. D.; Howard, D. K.; Oxman, J. D.; Upthagrove, A. L.; Quillen, S. L. *J. Am. Chem. Soc.* **1986,** *108,* 5964.

[7] Lewis, F. D.; Stern, C. L.; Yoon, B. A. *J. Am. Chem. Soc.* **1992,** *114,* 3131.

0022-3263/94/1959-2537$04.50/0

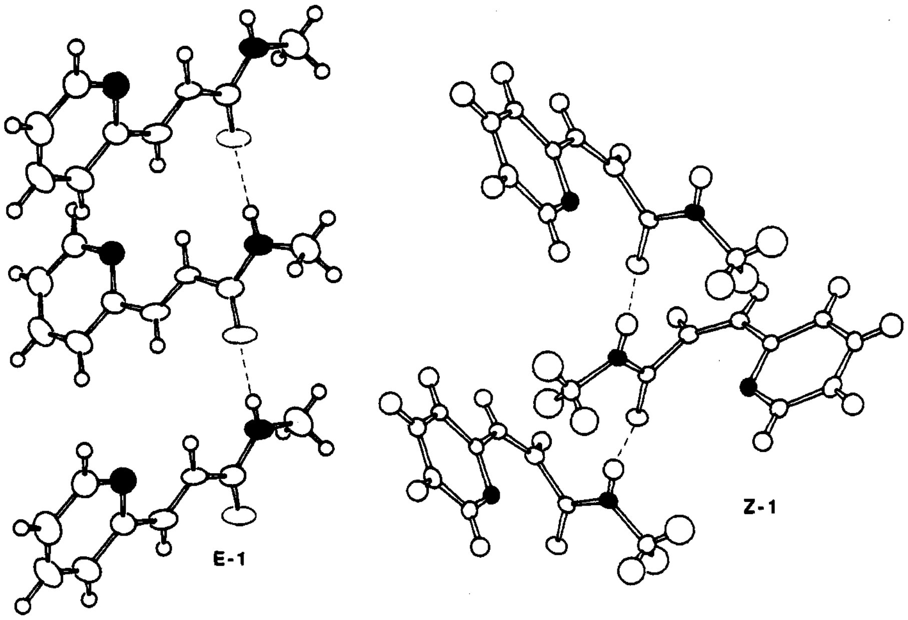

Figure 1. X-ray crystal structures for (*E*)- and (*Z*)-*N*-methyl-3-(2-pyridyl)propenamide.

hydrogen bonds, serves to elucidate the effects of inter- and intramolecular hydrogen bonding in these molecules.

Results and Discussion

Molecular Structure. The crystal structures of (*E*)-8 and several other *N*-methylamides have been investigated by Leiserowitz and Tuval[8a] and Rabinovich.[8b] Intermolecular hydrogen bonds connect chains of molecules generated via a glide plane. The phenyl–vinyl and vinyl–amide dihedral angles of (*E*)-8 are 18.5° and 4.8°, respectively, and the enone conformation is s-cis. As we have reported previously, the crystal structure of (*E*)-3 (Figure 1) is similar to that of (*E*)-8.[7] The smaller dihedral angles for (*E*)-3 (6.2° and 2.2°, respectively) vs (*E*)-8 presumably reflect the absence of nonbonded repulsion between the ortho and α-hydrogens in the s-cis vinylpyridine conformation. The crystal structure of (*Z*)-3 (Figure 1) is the first reported for the *Z* isomer of a cinnamic ester or amide. The phenyl–vinyl dihedral angle (6.7°) is similar to that for (*E*)-3 while the vinyl–amide dihedral angle (70.1°) is substantially larger than that for either (*E*)-1 or (*E*)-3. This unusually large dihedral angle permits the molecule to adopt the energetically favored glide motif for intramolecular hydrogen bonding in secondary amides. The pyridyl nitrogen in (*Z*)-3 is s-cis to the vinyl group, providing space for the nearly-orthogonal amide group. Nonbonded repulsion between the ortho hydrogen and the amide group would destabilize the analogous s-trans vinylpyridine conformer. For similar reasons neither (*Z*)-7 nor (*Z*)-8 can readily adopt a conformation similar to that of (*Z*)-3.

Structural data pertaining to the intermolecular hydrogen bonds in (*E*)-3, (*Z*)-3, and (*E*)-8 are summarized in Table 1. The N(H)···O distance for (*E*)-3 is slightly shorter than the average value of 2.85 Å for secondary amides,[8] while the values for (*Z*)-3 and (*E*)-8 are slightly longer. The N···C=O and C–N···O angles for (*E*)-3 are closer to the optimum values[8a,9] of 120° than are those for either (*Z*)-3 or (*E*)-8. These data suggest that intermolecular hydrogen bonding is energetically more favorable in the crystal structure of (*E*)-3 than in either (*Z*)-3 or (*E*)-8. Also reported in Table 1 are IR data for the N–H stretching frequency in the solid state and in CCl_4 solution and the difference between these values (Δν). The larger value of Δν for (*E*)-3 vs (*E*)-8 provides further evidence for a stronger intermolecular hydrogen bond in (*E*)-3. The negative value of Δν for (*Z*)-3 is indicative of hydrogen bond formation in solution as well as in the solid state (*vide infra*).

Table 1. Solid-State Intermolecular Hydrogen Bonding Geometries and N–H Stretching Frequencies for the 3-Pyridylpropenamides and *N*-Methylcinnamamide

	(*E*)-3	(*Z*)-3	(*E*)-8[d]
N··O distance[a]	2.82	2.88	2.89
N··C=O angle[b]	127.4	168.6	144.1
C–N··O angle[b]	121.4	130.6	110.4
phenyl-vinyl angle[b]	6.2	6.2	18.5
vinyl-amide angle[b]	2.2	70.1	4.8
ν_{N-H} (solid)[c]	3240[f]	3320[f]	3260[e]
ν_{N-H} (CCl_4)[c]	3450	3220	3440
$\Delta\nu_{N-H}$[c]	210	-100	180

[a] Distances in Å. [b] Angles in deg. [c] N–H stretching frequencies in cm^{-1}. [d] Data from ref 8. [e] Crystalline film. [f] Nujol mull.

A previous investigation of the structures of (*E*)-8 and (*Z*)-8 in solution established that (*E*)-8 adopts the same nearly planar enone s-cis conformation in solution as in the solid state, while (*Z*)-8 adopts a nonplanar enone s-trans conformation.[10] Selected solution-phase IR and ^1H NMR data for dilute (0.005 M) chlorocarbon solutions of the *E* and *Z* amides 3–8 are summarized in Table 2. Both the IR and ^1H NMR data for all of the *E* amides and for (*Z*)-7 and (*Z*)-8 are indicative of free (non-hydrogen bonded) amide N–H bonds. In comparison, the lower C=O and N–H stretching frequencies and larger N–H chemical shifts for (*Z*)-3–(*Z*)-6 are indicative of extensive hydrogen bonding. Since these data are concentration

---

[8] (a) Leiserowitz, L.; Tuval, M. *Acta Crystallogr.* **1978**, *B34*, 1230. (b) Rabinovich, D. *J. Chem. Soc. Sec. A* **1969**, 2361.

[9] Nakamoto, K.; Margoshes, M.; Rundle, R. E. *J. Am. Chem. Soc.* **1955**, *77*, 6480.

[10] Lewis, F. D.; Elbert, J. E., Upthagrove, A. L.; Hale, P. D. *J. Org. Chem.* **1991**, *56*, 553.

Table 2. IR Absorption and ^{1}H NMR Chemical Shift Data for the 3-Pyridylpropenamides

amide	$\nu_{C=O}$,[a] cm^{-1}	ν_{N-H},[a] cm^{-1}	δ_{N-H},[b] ppm
(*E*)-**3**	1680	3450	5.71 (8.25[c])
(*Z*)-**3**	1660	3220	11.25 (9.30[c])
(*E*)-**4**	1700	3524, 3406	5.65
(*Z*)-**4**	1669	3454, [d]	5.75, 11.35
(*E*)-**5**	1728, 1709	3405	8.40
(*Z*)-**5**	1717, 1684	3138	14.40
(*E*)-**6**	1691	3437	7.65
(*Z*)-**6**	1671	3080–2868[d]	14.10
(*E*)-**7**	1675	3450	6.22
(*Z*)-**7**	1677	3450	6.37
(*E*)-**8**	1668	3440	5.70
(*Z*)-**8**	1660	3460	5.08

[a] 0.005 M in CH_2Cl_2 or CCl_4 solution. [b] $CDCl_3$ unless otherwise noted. [c] Methyl sulfoxide-d_6. [d] The N–H and C–H stretches overlap.

independent, these *Z* amides must adopt the enone s-trans conformation and possess intramolecular hydrogen bonds in solution. Also reported in Table 2 are the ^{1}H NMR N–H chemical shifts for (*E*)-**3** and (*Z*)-**3** in the strong hydrogen bond acceptor solvent methyl sulfoxide. The observed chemical shifts are similar for the two isomers, indicative of similar intermolecular hydrogen bonding for both isomers.

Further evidence for a solvent-induced change in the conformation of (*Z*)-**3** is provided by an analysis of the NOE data obtained in $CDCl_3$ and methyl sulfoxide solution. Irradiation of the N–H hydrogen in $CDCl_3$ solution results in a small NOE for the α-vinyl hydrogen (0.9%) and a relatively large NOE for the aromatic hydrogen adjacent to the pyridyl nitrogen (6.3%). The reverse is observed in methyl sulfoxide solution for which N–H irradiation results in a large NOE for the α-vinyl hydrogen (8.3%) and a small NOE for the aromatic hydrogen (1.8%). These results support the assignment of intramolecular hydrogen bonded s-trans enone conformation for (*Z*)-**3** in $CDCl_3$ and an s-cis enone conformation for (*Z*)-**3** in methyl sulfoxide solution. Irradiation of the N–H of (*E*)-**3** results in large NOE's for the α-vinyl hydrogen and small NOE's for the aromatic hydrogen in $CDCl_3$ and methyl sulfoxide solution, in accord with an s-cis enone conformation in both solvents.

Energy-minimized structures for the s-cis conformer of (*E*)-**3** and the s-trans (hydrogen-bonded) and s-cis conformers of (*Z*)-**3** obtained using the MM2 force field are shown in Figure 2. Values for the vinyl-pyridyl and vinyl-amide carbon bond angles were taken from the crystal structures. Total energies and dihedral angles are indicated in Figure 2.[11] The significantly lower energy for (*E*)-**3** vs either conformer of (*Z*)-**3** is consistent with the observation that iodine atom-catalyzed isomerization provides a mixture of isomers containing >99% (*E*)-**3**.[12] The slightly lower calculated energy for the s-trans vs s-cis conformer is consistent with the observed preference for the former in solvents which do not disrupt the intramolecular hydrogen bond. It should be noted that the pyridyl–vinyl dihedral angle is significantly smaller for the s-trans vs s-cis conformer of (*Z*)-**3**. This difference may be responsible for the blue-shifted absorption maxima observed in very polar solvents (vide infra). The calculated intramolecular N(H)···N distance in the s-trans conformer of (*Z*)-**3** is 2.66 Å, somewhat shorter than the intermolecular N(H)···O distance observed in the solid state for either (*E*)-**3** or (*Z*)-**3**.

The recent investigations of the conformational preference of diamides by Gellman and co-workers[13] have established that the enthalpy of a single amide–amide hydrogen bond in a seven-membered ring (**9**) or larger rings is too small to overcome the torsional strain present in the hydrogen-bonded conformer. Introduction of an *E* alkene (but not a *Z* alkene) conformational control element in a nine-membered ring (**10**) results in predominant formation of the hydrogen-bonded conformer even in acetonitrile solution. The *Z* isomers of **1**–**3** exist exclusively as the hydrogen-bonded seven-membered ring conformers in nonpolar solvents. The *Z* alkenes serve as effective conformational control elements, limiting the total number of available conformations (two in (*Z*)-**1** and four in (*Z*)-**2** and (*Z*)-**3**) and determining their relative energies. In the case of (*Z*)-**3**, the hydrogen-bonded s-trans conformer is only slightly more stable than the s-cis conformer (Figure 2), and the hydrogen bond can be disrupted by methyl sulfoxide. Our preliminary studies of (*Z*)-**2** indicate that the hydrogen bond is not disrupted by methyl sulfoxide.[14] Further evidence for a much stronger hydrogen bond in (*Z*)-**2** vs (*Z*)-**3** is provided by proton or iodine-atom-catalyzed equilibria which provide predominantly (>99%) (*Z*)-**2**[5a] and (*E*)-**3**, respectively. This difference may reflect the smaller bond angles in the indole vs amide hydrogen bond acceptor which permits a more planar geometry for the hydrogen-bonded conformer. The *Z* isomer of methyl urocanate (**11**) also utilizes a five-membered heterocyclic hydrogen bond donor and is slightly more stable than its *E* isomer in dichloromethane solution.[6]

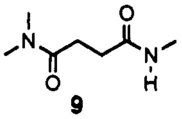

9

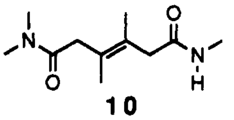

10

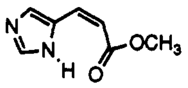

Z-**11**

The strength of the intramolecular hydrogen bond in the *Z* isomers of **3**–**6** might be expected to depend upon the *N*-alkyl substituent. On the basis of electron-donating or -withdrawing ability, the *N*-methyl- and *N*-phenylamides are expected to be weaker hydrogen bond donors than the primary amide and the imide a stronger hydrogen bond donor.[15] Unfortunately, the differences in IR and ^{1}H NMR data (Table 2) cannot be related directly to hydrogen bond strengths, and attempted iodine-atom-catalyzed thermal equilibration provides >99% *E* isomer from **3**–**6**.

Electronic Structure. UV absorption data for the *E* and *Z* isomers of **3**–**8** in dichloromethane solution are reported in Table 3. The spectra of (*E*)-**8** and (*Z*)-**8**, like those of other cinnamamides,[10] are dominated by a single broad absorption band, which was assigned by Fueno et

---

(11) (a) Burkert, U.; Allinger, N. L. *Molecular Mechanics*; ACS Monograph Series 177; American Chemical Society: Washington, DC, 1982. (b) Kundrot, C. E.; Ponder, J. W.; Richards, F. M. *J. Comput. Chem.* **1991**, *12*, 402.

(12) Yamashitu, S. *Bull. Chem. Soc. Jpn.* **1961**, *34*, 972.

(13) (a) Gellman, S. H.; Dado, G. P.; Liang, G.-B.; Adams, B. R. *J. Am. Chem. Soc.* **1991**, *114*, 1164. (b) Liang, G.-B.; Desper, J. M.; Gellman, S. H. *J. Am. Chem. Soc.* **1993**, *115*, 925.

(14) Lewis, F. D.; Yoon, B. A. Unpublished results.

(15) The relative hydrogen bond donor strength of amides vs imides remains a subject of debate: Jeong, K.-S.; Tjivikua, T.; Rebek, J. *J. Am. Chem. Soc.* **1990**, *112*, 3215.

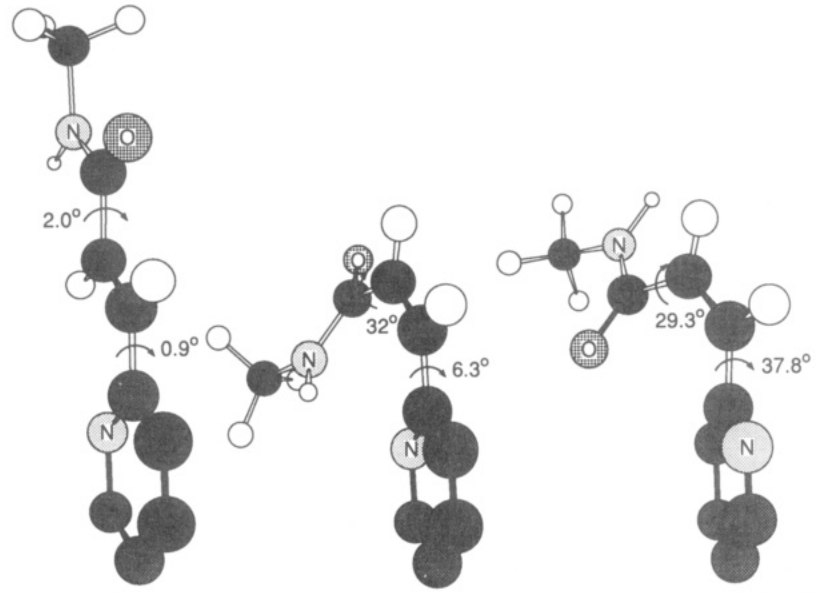

s-*cis* *E*-**3** (2.75) s-*trans* *Z*-**3** (7.79) s-*cis* *Z*-**3** (7.98)

Figure 2. Minimized MM2 structures of the lowest energy conformations of (*E*)- and (*Z*)-*N*-methyl-3-(2-pyridyl)propenamide. Energies shown in parentheses (kcal/mol).

Table 3. UV Absorption Data

amide[a]	solvent	λ_{max}	ϵ (λ_{max})
(*E*)-**3**	CH_2Cl_2	252, 292	16 800, 13 800
(*E*)-**3**	H_2O	250, 290	18 500, 18 700
(*Z*)-**3**	CH_2Cl_2	246, 286	14 700, 9500
(*Z*)-**3**	H_2O	238, 276	8800, 6200
(*E*)-**4**	CH_2Cl_2	250, 290	15 800, 13 200
(*Z*)-**4**	CH_2Cl_2	246, 288	14 800, 10 200
(*E*)-**5**	CH_2Cl_2	258, 296	11 800, 14 100
(*Z*)-**5**	CH_2Cl_2	250, 294	15 400, 11 600
(*E*)-**6**	CH_2Cl_2	254, 302	16 800, 22 600
(*Z*)-**6**	CH_2Cl_2	238, 286	21 100, 12 300
(*E*)-**7**	CH_2Cl_2	260, 290 (s)	17 900
(*Z*)-**7**	CH_2Cl_2	250, 285 (s)	9500
(*E*)-**8**	CH_2Cl_2	272	34 000
(*Z*)-**8**	CH_2Cl_2	255	11 000

[a] Data for 2.5–5.0 × 10^{-5} M amide.

al.[16] to a styrene-like allowed π,π^* transition on the basis of LCAO-SCF-CI calculations. The spectra of both the *E* and *Z* isomers of **3**–**7** display two absorption bands which partially overlap in the case of (*E*)-**7** and (*Z*)-**7** but are well-resolved in the case of (*E*)-**3** and (*Z*)-**3** (Figure 3). Comparison of the absorption data for the *E* and *Z* isomers of **3**–**6** indicates that N-substituents have only minor effects on the absorption maxima. However, the spectra of (*E*)-**6** and (*Z*)-**6** have long wavelength tails extending beyond 350 nm which are not present in the spectra of the other amides. Tailing is more pronounced for all of the *Z* vs *E* isomers. The pyridylpropenamides, like the cinnamamides,[10] are nonfluorescent at room temperature in solution. Weak emission is observed at 77 K in an EPA glass for both (*E*)-**3** and (*Z*)-**3** with 0,0 bands in emission and excitation ca. 330 nm.

In order to obtain further information about the singlet states of these molecules, we have performed INDO/S-SCF-CI (ZINDO) calculations for (*E*)-**3**, (*Z*)-**3**, and (*E*)-**8** using the algorithm developed by Zerner and co-workers.[17] The ZINDO-derived frontier molecular orbitals and orbital energies for these molecules are shown in Figure 4. The appearance and relative energies of the frontier orbitals for (*E*)-**8** are similar to those obtained for (*E*)-*N*,*N*-dimethylcinnamamide from restricted Hartree–Fock calculations performed using the GAUSSIAN 86 program package.[10] The appearance of the frontier orbitals for (*E*)-**3** and (*E*)-**8** is similar, differing mainly in the

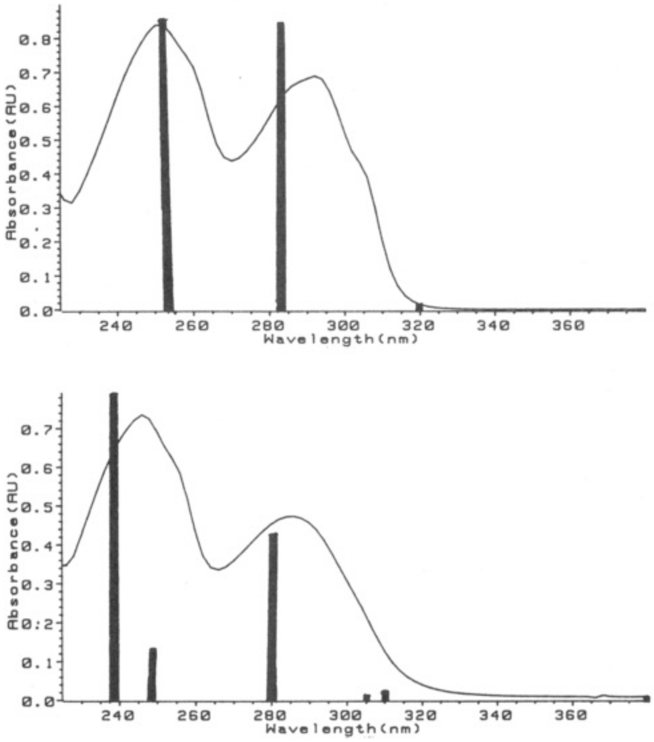

Figure 3. Electronic absorption spectra of 5 × 10^{-5} M (a) (*E*)- and (b) (*Z*)-*N*-methyl-3-(2-pyridyl)propenamide in dichloromethane solution. Vertical bars represent calculated energies and normalized oscillator strengths.

---

[16] Fueno, T.; Yamaguchi, K.; Naka, Y. *Bull. Chem. Soc. Jpn.* **1972**, *45*, 3294.

[17] (a) Bacon, A. D.; Zerner, M. C. *Theor. Chim. Acta* **1979**, *53*, 21. (b) Zerner, M. C.; Loew, G. H.; Kirchner, R. F.; Mueller-Westerhoff, U. T. *J. Am. Chem. Soc.* **1980**, *102*, 589. (c) Ridley, J.; Zerner, M. *Theor. Chim. Acta* **1973**, *32*, 111. (d) Anderson, W. P.; Edwards, W. D.; Zerner, M. C. *Inorg. Chem.* **1986**, *25*, 2728.

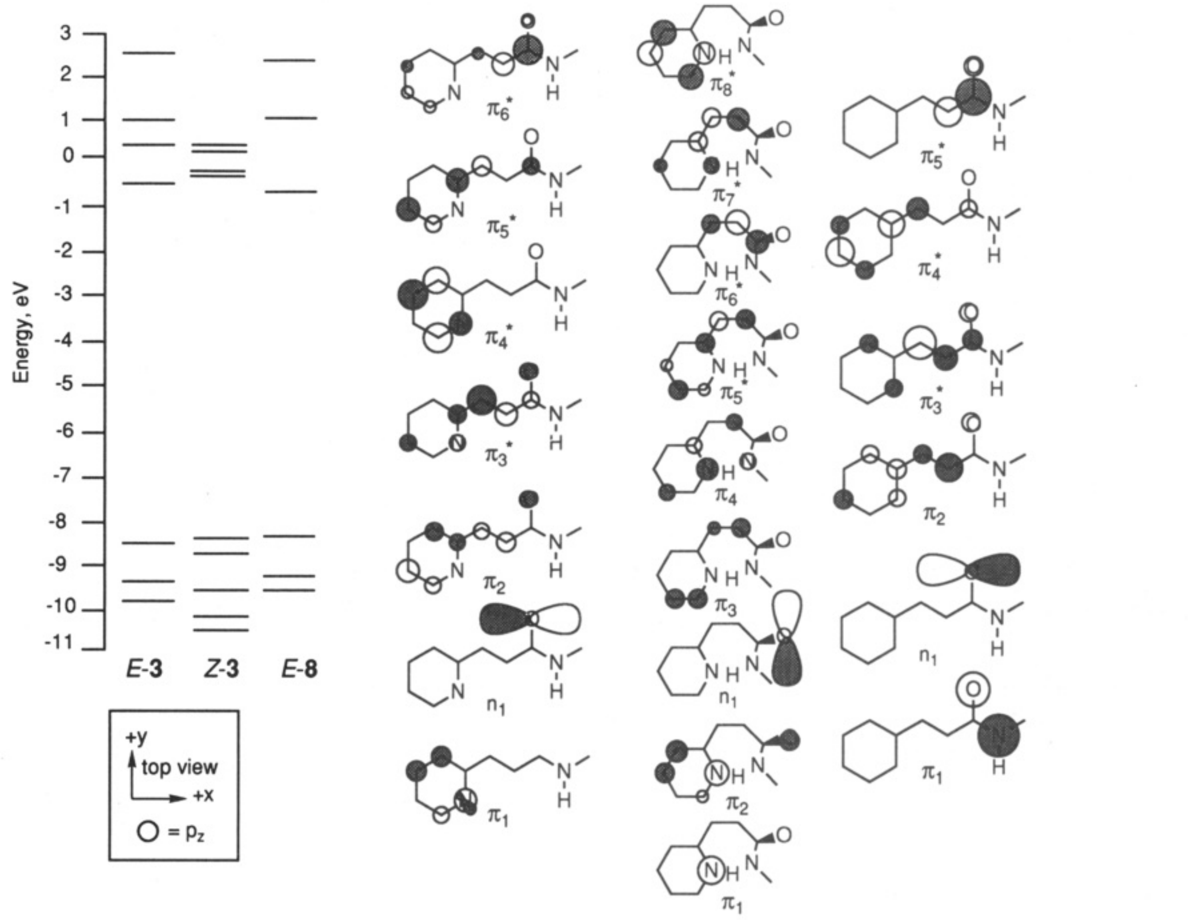

Figure 4. Frontier molecular orbitals for (*E*)- and (*Z*)-*N*-methyl-3-(2-pyridyl)propenamide and (*E*)-*N*-methylcinnamamide.

occurrence of the pyridine lone pair (n_1) as the fifth highest filled orbital for (*E*)-**3** and in the symmetries of the HOMOs.[18] The ionization energy of the pyridine n orbital lies well above that of the highest occupied π orbitals in the photoelectron spectrum of 2-vinylpyridine.[19] The energies of the two highest occupied and four lowest unoccupied orbitals are much more closely spaced for (*Z*)-**3** than is the case for (*E*)-**3** or (*E*)-**8**, and the appearance of the frontier orbitals is radically different (Figure 4).

Table 4. Calculated Absorption Maxima (λ_{max}), Oscillator Strengths (*f*), and Configuration Interaction (CI) of Excited Singlet States (S) of the 3-Pyridylpropenamides and *N*-Methylcinnamamide

amide	excited state	λ_{max}, nm (*f*)	CI (%) and character
(*E*)-**3**	S_1	380 (0.001)	64 $n_1 \rightarrow \pi_3$
			18 $n_1 \rightarrow \pi_5$
			10 $n_1 \rightarrow \pi_6$
	S_3	284 (0.486)	64 $\pi_2 \rightarrow \pi_3$
			20 $\pi_2 \rightarrow \pi_4$
	S_4	254 (0.494)	14 $\pi_1 \rightarrow \pi_3$
			34 $\pi_2 \rightarrow \pi_3$
			37 $\pi_2 \rightarrow \pi_4$
(*Z*)-**3**	S_2	311 (0.010)	36 $n_1 \rightarrow \pi_5$
			31 $n_1 \rightarrow \pi_7$
			18 $n_1 \rightarrow \pi_8$
			6 $\pi_3 \rightarrow \pi_5$
	S_4	279 (0.252)	7 $\pi_1 \rightarrow \pi_6$
			21 $\pi_3 \rightarrow \pi_5$
			18 $\pi_3 \rightarrow \pi_6$
			36 $\pi_4 \rightarrow \pi_5$
	S_6	237 (0.466)	32 $\pi_3 \rightarrow \pi_5$
			19 $\pi_3 \rightarrow \pi_6$
			26 $\pi_4 \rightarrow \pi_7$
			7 $\pi_2 \rightarrow \pi_5$
(*E*)-**8**	S_1	342 (0.000)	74 $n_1 \rightarrow \pi_3$
			13 $n_1 \rightarrow \pi_4$
			14 $n_1 \rightarrow \pi_5$
	S_2	301 (0.944)	96 $\pi_2 \rightarrow \pi_3$
	S_4	238 (0.094)	92 $\pi_1 \rightarrow \pi_3$
			5 $\pi_1 \rightarrow \pi_4$

The calculated absorption maxima, oscillator strengths, and character of selected excited singlet states of (*E*)-**3**, (*Z*)-**3**, and (*E*)-**8** obtained from ZINDO calculations are reported in Table 4.[18] As shown by the vertical bars in Figure 3, the calculated and observed absorption maxima for (*E*)-**3** and (*Z*)-**3** are in reasonable agreement. In the case of (*E*)-**8** the only low energy allowed transition is the essentially pure HOMO → LUMO, $\pi \rightarrow \pi^*$ transition (S_2). The $\pi_N \rightarrow \pi^*$ transition (S_4), which was previously suggested as a possible unreactive low-energy singlet state for *N,N*-dimethylcinnamamide,[10] occurs at higher energy and has a lower calculated oscillator strength than S_2. Both (*E*)-**3** and (*Z*)-**3** have two low-energy allowed transitions which result from configuration interaction between two or more $\pi \rightarrow \pi^*$ transitions. In the case of (*E*)-**3** configuration interaction between the strongly allowed HOMO → LUMO and weakly allowed HOMO → SLUMO transitions results in two transitions (S_3 and S_4) of comparable calculated oscillator strength. Two allowed $\pi \rightarrow \pi^*$ transitions are also observed for 2-vinylpyridine.[20] Even more extensive configuration interaction is encountered in the two allowed $\pi \rightarrow \pi^*$ transitions of (*Z*)-**3** (S_4

---

[18] A more complete set of molecular orbitals and description of excited singlet states is provided as supplementary material.

[19] Modelli, A.; Distefano, G. *J. Electron Spect. Rel. Phenom.* **1981**, *23*, 323.

[20] Gamba, A.; Tantardini, G. *Gazz. Chim. Ital.* **1974**, *104*, 857.

Table 5. Quantum Yields and Optimum Conversions for Photoisomerization

amide	solvent	$\Phi_{E,Z}$	$\Phi_{Z,E}$	% Z^a
3	CH_2Cl_2	0.31	$<10^{-3}$	99
	CH_3CN	0.22	$<10^{-3}$	98
	H_2O		$<10^{-3}$	99
	THF	0.05	0.07	*b*
	CH_3CH_2OH	0.12	0.04	*b*
	CH_3OH	0.14	0.011	*b*
	$(CH_3)_2SO$	0.06	0.06	77
4	CH_2Cl_2	0.18	<0.01	93^c
	CH_3OH	0.11		
	$(CH_3)_2SO$	0.09		
5	CH_2Cl_2	0.59	<0.01	93^c
	CH_3OH	0.31		
6	CH_2Cl_2	0.01	0.001	65
7	CH_2Cl_2	0.16	0.28	65
	H_2O			62
	$(CH_3)_2SO$	0.02	0.08	77
8	CH_2Cl_2	0.034	0.27	40
	MeOH	0.14		
	$(CH_3)_2SO$	0.019		

[a] % *Z* isomer obtained upon prolonged 313-nm irradiation of either *E* or *Z* isomer, except as noted. [b] Amides are unstable to prolonged irradiation in these solvents. [c] Conversion of *E* to *Z* isomers.

and S_6). The observed increase in configuration interaction between $\pi \rightarrow \pi^*$ transitions for amides (*E*)-**8** < (*E*)-**3** < (*Z*)-**3** results from a decrease in the energetic separation of the π orbitals in this series, as observed by Platt[21] for polynuclear aromatic hydrocarbons and Lewis et al.[22] for nickel(II) and palladium(II) bis(β-diketonates).

In addition to allowed $\pi \rightarrow \pi^*$ transitions, ZINDO predicts the existence of forbidden (low oscillator strength) low-energy $n \rightarrow \pi^*$ transitions for (*E*)-**3**, (*Z*)-**3**, and (*E*)-**8** (S_1, S_2, and S_1, respectively). Extensive configuration interaction involving transitions from the oxygen lone pair orbital to several π^* orbitals is responsible for the low energy of these transitions. The other low-energy states of (*E*)-**3** (S_2 and S_3) and (*Z*)-**3** (S_1 and S_3) also display extensive configuration interaction and low oscillator strengths. These low-energy singlet states are not observed in the electronic absorption spectra, but may be obscured by the broad allowed $\pi \rightarrow \pi^*$ transitions (Figure 3). Internal conversion from initially populated $\pi \rightarrow \pi^*$ states to lower energy $n \rightarrow \pi^*$ states could account for the absence of room-temperature fluorescence from these molecules as well as their photochemical behavior (*vide infra*). It should be noted that these calculations have been performed for vertical excited states. Twisting about the C=C bond or other geometric changes will, no doubt, result in changes in the energies of the excited singlet states.

Photoisomerization. Neither (*E*)-**3** nor (*Z*)-**3** undergoes photoisomerization in the solid state. Quantum yields for photoisomerization of amides **3**–**8** determined using 313-nm irradiation in several solvents are summarized in Table 5. Also reported is the % *Z* isomer content of the isomer mixtures obtained upon prolonged irradiation of either the *E* or *Z* isomer. In cases where the values of both $\Phi_{E,Z}$ and $\Phi_{Z,E}$ are moderately large (e.g., (*E*)-**7** or (*E*)-**8** in dichloromethane solution) the isomer mixture obtained is in good agreement with the calculated photostationary state (eq 4). Very high conversions of *E* to *Z* isomers are observed for **3**–**5**. Since the *E* and *Z* isomers of **3**–**5** have comparable absorbances at 313 nm, values of $\Phi_{Z,E}$ must be very small for (*Z*)-**4** and (*Z*)-**5**, as is the case for (*Z*)-**3**.

$$\frac{[Z]}{[E]} = \frac{\phi_{E,Z}\,\epsilon_E}{\phi_{Z,E}\,\epsilon_Z} \qquad (4)$$

Upper bounds for these values estimated using the observed isomer content, molar absorbances, and $\Phi_{E,Z}$ values are reported in Table 4. While the quantum yield for isomerization of (*Z*)-**6** is also very low, high $E \rightarrow Z$ conversions are not observed due to the low quantum yield for isomerization of (*E*)-**6**.

Values of $\Phi_{Z,E}$ for amides **3**–**6**, which form intramolecular hydrogen bonds in dichloromethane solution, are small while those for amides **7** and **8**, which cannot form intramolecular hydrogen bonds, are moderately large (Table 5). A further indication of the relationship between hydrogen bonding and photoisomerization efficiency is provided by the effect of solvent upon the values of $\Phi_{Z,E}$ for (*Z*)-**3**. No isomerization is observed in dichloromethane, acetonitrile, or water, while moderately efficient isomerization is observed in THF, methanol, ethanol, and methyl sulfoxide. NOE studies of (*Z*)-**3** indicated that the intramolecular hydrogen bond is broken in methyl sulfoxide solution. While the solvent dependence of $\Phi_{Z,E}$ for (*Z*)-**3** cannot be readily correlated with standard solvent polarity scales, it can be roughly correlated with the Taft solvatochromic β parameter (hydrogen bond acceptor strength).[23] Photoisomerization is observed only in solvents with β values comparable to or greater than that for pyridine ($\beta = 0.64$). Thus, while water is more polar and a stronger hydrogen bond donor than methanol or ethanol, it is a weaker hydrogen bond acceptor than pyridine, whereas methanol and ethanol are stronger hydrogen bond acceptors than pyridine. It is also possible that the free energy of solvation of the amide carbonyl group by water is actually larger for the more exposed s-trans vs s-cis conformation of (*Z*)-**3**. While photoisomerization cannot be observed for (*Z*)-**3** at room temperature in dichloromethane solution, it can be detected at elevated temperatures. Values of $\Phi_{Z,E}$ determined in both dichloromethane and methyl sulfoxide solution at several temperatures in a constant volume, high pressure cell are reported in Table 6. The values obtained in dichloromethane solution are observed to increase with increasing temperature, while the data obtained in methyl sulfoxide solution show no discernable trend.

Values of $\Phi_{E,Z}$ are also dependent upon amide structure and solvent (Table 5). Amides **3**–**5** and **7** have larger values of $\Phi_{E,Z}$ in dichloromethane solution than do amides **6** and **8**. We previously proposed that the low value of $\Phi_{E,Z}$ for **8** might be due to the presence of a unreactive singlet state at lower energy than the spectroscopically observed π,π^* singlet state.[10] The long-wavelength tail present in the absorption spectrum of (*E*)-**7** suggests the presence of a low-energy singlet state of low oscillator strength in this amide as well. While the results of ZINDO calculations for (*E*)-**8** (Table 4) appear to corroborate this suggestion, they also indicate the presence of a low-energy n,π^* state for (*E*)-**3**, which has a moderately large value of $\Phi_{E,Z}$. In the absence of fluorescence from any of these amides, direct spectroscopic characterization of the lowest singlet state is not possible. Values of $\Phi_{E,Z}$ for **3**–**5** and **7** decrease as the hydrogen bonding strength of the solvent increases. In view of the highly polar nature of the amide group it

---

[21] Platt, J. R. *J. Chem. Phys.* **1950**, *18*, 1168.

[22] Lewis, F. D.; Salvi, G. D.; Kanis, D. R.; Ratner, M. A. *J. Inorg. Chem.* **1993**, *32*, 1251.

[23] Kamlet, M. J.; Abboud, J.-L. M.; Abraham, M. H.; Taft, R. W. *J. Org. Chem.* **1983**, *48*, 2877.

Table 6. Temperature Dependence of Quantum Yield for Photoisomerization of (*Z*)-*N*-methyl-3-(3-pyridyl)propenamide

T, K	$\Phi_i{}^{a,c}$	$\Phi_i{}^{b,c}$
308		0.036
323		0.049
343	0.010	0.044
363	0.013	
373	0.015	0.049
383	0.017	
393	0.019	0.042

[a] 0.005 M dichloromethane solutions. [b] 0.005 M methyl sulfoxide solutions. [c] Irradiation with 300-nm light.

is possible that strong solvation of the excited singlet results in a solvent-induced barrier for twisting about the double bond. Alternatively, hydrogen bonding may result in reordering the energies of the singlet excited states, as previously noted for 2-vinylpyridine by Del Bene.[24]

Triplet-sensitized (Michler's ketone) irradiation of (*E*)-**3** or (*Z*)-**3** in dichloromethane solution results in an isomer mixture containing 52% (*Z*)-**3**. This indicates that the excited singlet (*Z*)-**3** does not undergo intersystem crossing in competition with nonradiative decay to the ground state. The temperature dependence of the isomerization of (*Z*)-**3** in dichloromethane solution (Table 6) is indicative of an activated isomerization process. This is more likely due to a barrier to twisting on the singlet surface than to intersystem crossing, which is an unactivated process for other aryl olefins.[25] The photoisomerization efficiency of (*E*)-**3** is unaffected by either oxygen saturation or addition of 0.1 M cyclohexadiene, a good triplet quencher. Thus, isomerization of (*E*)-**3** apparently occurs via a short-lived (<0.1 ns) singlet or triplet state.

The simplest interpretation of the photochemical behavior of (*E*)-**3** and (*Z*)-**3** is provided by the singlet-state potential energy diagram shown in Figure 5a which is based on the potential energy diagram for stilbene and styrene isomerization.[25] The calculated 5 kcal/mol difference between ground-state isomers is consistent with the observation of essentially quantitative iodine-atom catalyzed $Z \rightarrow E$ isomerization. The vertical excitation energies of the isomers are similar (Table 3). The barrier for the exergonic conversion of planar excited (*E*)-**3** to a twisted singlet is presumably small. The singlet excited s-trans (hydrogen bonded) and s-cis conformers of (*Z*)-**3** are of comparable energy and must both lie well above the twisted singlet. The temperature dependence of the isomerization quantum yields (Table 6) indicates the presence of a significantly larger barrier for twisting of the s-trans vs s-cis conformer of (*Z*)-**3** (Figure 5a). The apparent origin of the larger barrier is the intramolecular hydrogen bond which must be broken in order to form the twisted singlet.

The potential energy surface proposed for **3** differs in several important respects from that recently proposed by Arai et al.[5b] for **2** (Figure 5b). In the case of **2** the *Z* isomer is thermodyamically more stable than the *E* isomer and also has a lower vertical excitation energy. The planar excited single state may therefore lie below the twisted singlet, rendering isomerization endergonic irrespective of the presence or absence of an enhanced barrier for twisting due to the intramolecular hydrogen bond. Finally, it should be noted that intramolecular hydrogen bonding is not a sufficient condition for one-way photoisomerization. The *E* and *Z* isomers of methyl urocanate (**11**) are of comparable thermodynamic stability due to intramolecular hydrogen bonding in the *Z* isomer. While the *Z* isomer has a lower vertical excitation energy, both isomers undergo efficient photoisomerization ($\Phi_{E,Z} = 0.63$ and $\Phi_{Z,E} = 0.33$ in dichloromethane solution).[6] The effects of inter- and intramolecular hydrogen bonding on photoisomerization processes are under continuing investigation in our laboratory.

Experimental Section

^{1}H NMR spectra were recorded on Varian XLA 400 and Varian Gemini 300 spectrophotomers in $CDCl_3$ and methyl sulfoxide-d_6 solvents with TMS as an internal standard. NOE difference spectra experiments were performed on the Varian XLA 400 using samples degassed by four freeze–pump–thaw cycles. UV–vis absorption spectra were measured with a Hewlett-Packard Model 8452A diode array spectrophotometer in 1-cm-pathlength quartz cuvettes. Infrared spectra of 0.005 M solutions of amides in dichloromethane and carbon tetrachloride were recorded in 1-mm-pathlength NaCl cells using a Perkin-Elmer Model 286 double beam or Mattson FT-IR spectrophotometer. Low-temperature emission spectra were obtained through a nitrogen-cooled fluorescence dewar with a hanging finger window. Solutions were approximately 10^{-4} M and purged with nitrogen >5 min in quartz epr tubes.

Mass spectra were determined with a Hewlett-Packard 5985 GC/VG70-250SE MS system using an ionizing voltage of 70 eV. Product ratios were analyzed with Hewlett-Packard 5890 A or Varian 3700 chromatographs equipped with 10 m × 0.53 mm capillary columns coated with poly(dimethylsiloxane) or poly(methylphenylsiloxane).

The light sources were a Rayonet reactor equipped with 254- or 300-nm lamps, a Hanovia 450-W high-pressure mercury arc lamp with merry-go-round apparatus with Pyrex filter (>300-nm bandpass) or Pyrex and potassium chromate solution filter (313-nm bandpass), or an Oriel optical bench equipped with a 200-W high-pressure mercury–xenon lamp and a Bausch and Lomb high-intensity monochromator set at the desired wavelength.

Photoisomerization quantum yields and *E,Z* photoequilibria were determined for 3-mL aliquots of 0.005 M solutions of amides contained in 13-mm-o.d. quartz or Pyrex test tubes sealed with white rubber septa, and purged >5 min with dry nitrogen. Samples to be irradiated under oxygen were bubbled with dry oxygen for 5 min. Samples were irradiated in triplicate with light from the Rayonet reactor or Hanovia lamp. Quantum yields were analyzed for isomer formation at <10% conversion with *trans*-stilbene as the actinometer.[21]

Temperature-dependent quantum yields were determined at 35–120 °C. The 1–1.2-mL solutions were purged for 10 min with dry nitrogen and transferred in a glovebox to a stainless steel cell with a single sapphire window capable of withstanding high pressure[25] and equipped with a magnetic stirrer. The cell was heated to a constant temperature with an Oxford Model ITC4 temperature controller and then irradiated on an optical bench with 300-nm light.

Data for X-ray crystal structures were collected on an Enraf-Nonius CAD4 automated ok-axis diffractometer with graphite-monochromated Mo Kα radiation. Crystallographic data for (*E*)-**3**: mp 108–110 °C, orthorhombic; space group *Pbca*, a = 9.370(3) Å, b = 11.003(2) Å, c = 16.906 Å, V = 1743(1) Å^3, Z = 8, m_{calcd} = 0.78 cm^{-1}, r_{calcd} = 1.236 g/cm^3; 2192 unique reflections, R = 0.045, R_w = 0.044. (*Z*)-**3**: mp 72–74 °C; monoclinic; space group *P*21/*c*, a = 10.838(2) Å, b = 8.712(2) Å, c = 9.849(4) Å, V = 838.6(5) Å^3, Z = 4, m_{calcd} = 0.81 cm^{-1}, r_{calcd} = 1.284 g/cm^3; 1826 unique reflections, R = 0.038, R_w = 0.049.

Methods of Calculation. The INDO/S-SCF-CI (ZINDO) calculations for (*E*)-**3**, (*Z*)-**3**, and (*E*)-**8** were performed by a method developed by Zerner and co-workers[17] and implemented as described by Lewis et al.[22] The geometry for (*E*)-**3** was taken from X-ray crystal data. The bond lengths and bond angles for

---

(24) Del Bene, J. E. *Chem. Phys.* **1980**, *50*, 1.

(25) Lewis, F. D.; Bassani, D. M. *J. Am. Chem. Soc.* **1993**, *115*, 7523.

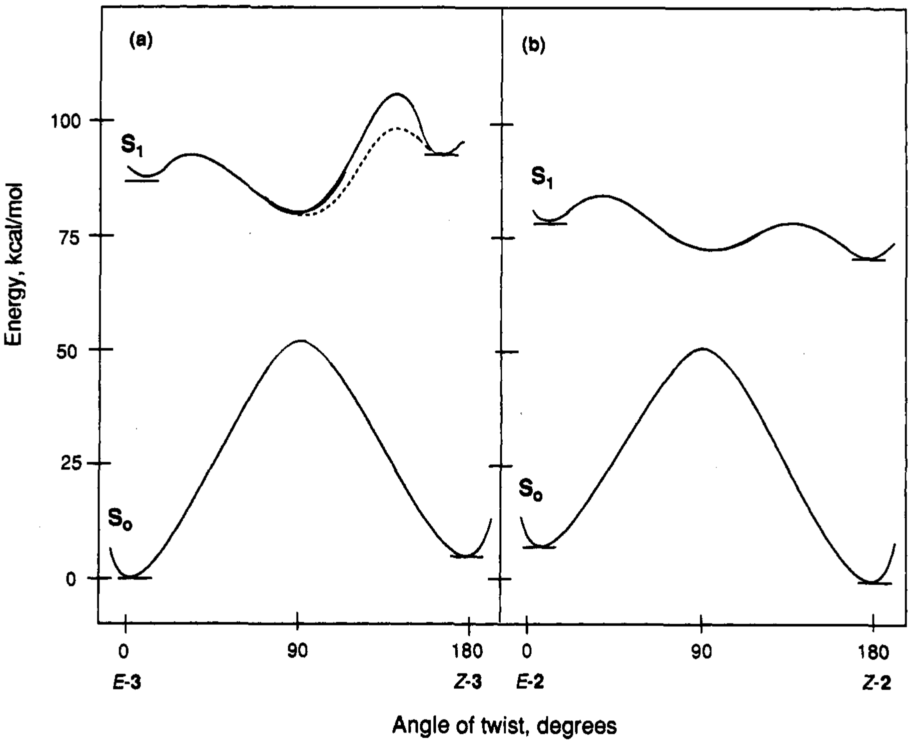

Figure 5. Potential energy surfaces (a) for the photoisomerization of **3** in nonpolar (solid line) and methyl sulfoxide (broken line) solution and (b) for the photoisomerization of **2** (after Arai et al.[5b]).

(*Z*)-**3** were taken from the X-ray crystal structure and then minimized by MM2.[11] The ZINDO calculations were performed a Stellar mini supercomputer and required approximately 5–10 min of CPU time.

Materials. All solvents were spectral grade (Aldrich or Fisher). Acetonitrile and dichloromethane were distilled over calcium hydride prior to use. THF was distilled over Na/benzophenone ketyl. Ethyl alcohol was fractionally distilled over KOH. Methyl alcohol, isopentane, and ethyl ether were used as received. Methyl sulfoxide was distilled over $NaNH_2$. *trans*-Stilbene (Aldrich) was recrystallized two times from benzene and once from ethyl alcohol. All other compounds were used as received unless otherwise directed.

(*E*)-Ethyl 3-(2-Pyridyl)propenoate and (*E*)-Ethyl 3-(2-Pyridyl)propenoate. The ethyl 3-pyridylpropenate precursors to amides **3-7** were synthesized from pyridinecarboxaldehydes (Aldrich) via a Wittig reaction in 80% yield.[26] Mixtures of *E* and *Z* isomers were converted to the pure *E* isomer (>99%) by iodine-atom-catalyzed isomerization.[12]

(*E*)-*N*-Methyl-3-pyridylpropenamides (*E*)-3 and (*E*)-7 and (*E*)-3-(2-Pyridyl)propenamide ((*E*)-4). The appropriate ethyl ester prepared above was converted to the amides using a modified version of the Weinreb reaction.[27] A suspension of dry dichloromethane and 3 equiv of methylamine hydrochloride or ammonium chloride (Aldrich) was cooled to 0 °C under nitrogen atmosphere. A solution of 3 equiv of 2 M trimethylaluminum in hexanes (Aldrich) was slowly added. When gas evolution had ceased, the solution was allowed to warm to room temperature and stirred for 30 min. A solution of 2 equiv of ester in dichloromethane was added and stirred for 3 days. The solution was quenched with water and filtered. The aqueous layer was basified with K_2CO_3, extracted with dichloromethane, and dried over $MgSO_4$. Recrystallization in ethyl acetate/hexane afforded white needle-like crystals in up to 45% yields. (*E*)-**3**: ^{1}H NMR ($CDCl_3$) δ 2.96 (d, 3 H), 5.71 (bs, 1 H), 6.97 (d, $J = 15.2$ Hz, 1 H), 7.25 (t, 1 H), 7.37 (d, 1 H), 7.62 (d, $J = 15.2$ Hz, 1 H), 7.70 (t, 1 H), 8.62 (d, 1 H); ^{1}H NMR (DMSO-d_6) δ 2.71 (d, 3 H), 7.05 (d, $J = 15.2$ Hz, 1 H), 7.36 (m, 1 H), 7.43 (d, $J = 15.2$ Hz, 1 H), 7.58 (m, 1 H), 7.83 (m, 1 H), 8.25 (br d, 1 H), 8.60 (d, 1 H); IR (CH_2Cl_2) 3450, 1680, 1640, 1580. (*E*)-**4**: mp 145-147 °C; ^{1}H NMR ($CDCl_3$) δ 5.65 (br s, 2 H), 7.04 (d, $J = 14.6$ Hz, 1 H), 7.29 (m, 1 H), 7.38 (d, 1 H), 7.65 (d, $J = 14.6$ Hz, 1 H), 7.73 (t, 1 H), 8.63 (d, 1 H); IR (CH_2Cl_2) 3524, 3406, 1700, 1641 cm^{-1}. (*E*)-**7**: mp 101–103 °C; ^{1}H NMR ($CDCl_3$) δ 2.95 (d, 3 H), 6.22 (br s, 1 H), 6.54 (d, $J = 17.0$ Hz, 1 H), 7.32 (m, 1 H), 7.62 (d, $J = 17.0$ Hz, 1 H), 7.79 (d, 1 H), 8.56 (d, 1 H), 8.74 (d, 1 H); IR (CH_2Cl_2) 3450, 1675, 1633, 1524 cm^{-1}.

(*E*)-*N*-Acetyl-3-(2-pyridyl)propenamide ((*E*)-5). The secondary amide (*E*)-**4** was converted to the imide using the method of Davidson and Skovronek.[28] To a solution of 1 equiv of (*E*)-**4** in 2 mL of acetic anhydride (Mallinckrodt) was added ~0.2 mL (1.1 equiv) of concentrated H_2SO_4. The reaction mixture was subsequently heated at 90 °C and stirred for 1 h. Quenching with ice was followed by addition of K_2CO_3 to attain a pH of 8. Extraction with dichloromethane and drying over $MgSO_4$ yielded 31% of the tan solid: mp 142–144 °C; ^{1}H NMR ($CDCl_3$) δ 2.51 (s, 3 H), 7.24 (d, $J = 15.2$ Hz, 1 H), 7.31 (m, 1 H), 7.45 (d, 1 H), 7.74 (m, 1 H), 7.79 (d, $J = 15.2$ Hz, 1 H), 8.4 (bs, 1 H), 8.67 (d, 1 H). IR (CH_2Cl_2 or CCl_4) 3405, 1728, 1709, 1690, 1641 cm^{-1}; MS *m/e* 190 (M^+, 32), 162 (50), 147 (69), 132 (100), 120 (39), 104 (63), 78 (53).

(*E*)-*N*-Phenyl-3-(2-pyridyl)propenamide ((*E*)-6). A methanolic solution of 1 equiv of ethyl 3-(2-pyridyl)propenoate and 1.5 equiv of aniline (Baker) was added to a solution of 1.1 equiv of sodium methoxide/methanol and stirred under N_2 atmosphere for 3 days. After the solvent was removed, dichloromethane was added and then extracted with 5% HCl solution. The aqueous solution was neutralized with sodium bicarbonate and extracted with dichloromethane. Drying over $MgSO_4$ and recrystallization from ethyl acetate/hexane yielded 17% of a flaky white solid: mp 149–152 °C; ^{1}H NMR ($CDCl_3$) δ 7.10–7.90 (ar, 10 H), 7.62 (bs, 1 H), 8.64 (d, 1 H). IR (CCl_4) 3437, 1691, 1642 cm^{-1}; MS *m/e* 223 (M^+), 132 (100), 104 (31), 93 (22), 78 (29).

Preparation of *Z* Isomers of 3-7. The 0.005 M solutions of the *E* isomers of **3-7** were irradiated in Pyrex vessels with a Hanovia 450-W high-pressure mercury arc lamp to the photostationary state. The solvent was removed, and the residues of **3**, **4**, **6**, and **7** were purified by silica gel column chromatography

---

[26] Sugasawa, S.; Matsuo, H. *Chem. Pharm. Bull.* **1960**, *8*, 819.

[27] (a) Lipton, M. F.; Basha, A.; Weinreb, S. M. *Org. Synth.* **1981**, *59*, 49. (b) Barrett, A. G. M.; Dashyant, D. *Tetrahedron Lett.* **1987**, *28*, 3327.

[28] Davidson, D.; Skovronek, H. *J. Am. Chem. Soc.* **1958**, *80*, 376.

or preparative thin-layer chromatography. The elutants were as follows: for **3** and **7**, 5% methanol in chloroform (basified with NH_4OH); for **4**, 10% methanol in chloroform (rendered basic by addition of NH_4OH); and for **6**, 10% hexane in chloroform. (*Z*)-**5** was unstable to silica chromatography. The *Z* isomers of **3**, **4**, and **7** are crystalline solids while (*Z*)-**5** and (*Z*)-**6** are oils. (*Z*)-**3**: ^{1}H NMR ($CDCl_3$) δ 2.92 (d, 3 H), 6.16 (d, *J* = 13.6, 1 H), 6.65 (d, *J* = 13.6 Hz, 1 H), 7.30 (t, 1 H), 7.39 (d, 1 H), 7.79 (m, 1 H), 8.64 (d, 1 H), 11.25 (bs, 1 H); ^{1}H NMR (DMSO-d_6) δ 2.66 (d, 3 H), 6.74 (d, *J* = 13.6 Hz, 1 H), 6.13 (d, *J* = 13.6 Hz, 1 H), 7.33 (d, 1 H), 7.81 (m, 1 H), 7.32 (m, 1 H), 8.59 (d, 1 H), 9.3 (br s, 1 H); IR (CCl_4) 3220, 1660, 1610 cm^{-1}. (*Z*)-**4**: mp 52–56 °C; ^{1}H NMR ($CDCl_3$) δ 5.75 (br s, 1 H), 6.13 (d, *J* = 13.8 Hz, 1 H), 6.74 (d, *J* = 13.8 Hz, 1 H), 7.34, (m, 1 H), 7.81 (m, 1 H), 8.60 (d, 1 H), 8.41 (d, 1 H), 11.35 (br s, 1 H); IR (CH_2Cl_2 or CCl_4) 3454, 1669, 1641, 1587 cm^{-1}. (*Z*)-**5**: ^{1}H NMR ($CDCl_3$) δ 2.50 (d, 3 H), 6.14 (d, *J* = 13.9 Hz, 1 H), 6.80 (d, *J* = 13.9 Hz, 1 H), 7.35–7.44 (m, 2 H), 7.86 (t, 1 H), 8.75 (d, 1 H), 14.4 (br s, 1 H); IR (CCl_4) 3138, 1717, 1684 cm^{-1}. (*Z*)-**6**: ^{1}H NMR ($CDCl_3$) δ 6.25 (d, *J* = 14.0 Hz, 1 H), 6.73 (d, *J* = 14.0 Hz, 1 H), 7.32 –7.46 (m, 4 H), 7.40 (d, 1 H), 7.77 (m 1 H), 7.86 (m, 1 H), 7.10 (m, 1 H), 8.75 (m, 1 H), 14.15 (br s, 1 H); IR (CCl_4) 3077, 3028, 1671, 1622 cm^{-1}. (*Z*)-**7**: mp 56–59 °C; ^{1}H NMR ($CDCl_3$) δ 2.82 (d, 3 H), 6.08 (d, *J* = 12.4 Hz, 1 H), 6.37 (bs, 1 H), 6.66 (d, J = 12.4 Hz, 1 H), 7.26 (m, 1 H), 8.02 (d, 1 H), 8.47 (d, 1 H), 8.55 (s, 1 H); IR (CH_2Cl_2 or CCl_4) 3450, 1667, 1524 cm^{-1}.

Acknowledgement is made to the donors of the Petroleum Research Fund, administered by the American Chemical Society, for the support of this research.

Supplementary Material Available: ^{1}H NMR spectra (8 pages). This material is contained in libraries on microfiche, immediately follows this article in the microfilm version of the journal, and can be ordered from the ACS; see any current masthead page for ordering information.